

# Astrocytes and diffusive spread of substances in brain extracellular space

**Ang D. Sherpa<sup>1,2,\*</sup> and Sabina Hrabetova<sup>1</sup>**

<sup>1</sup> Department of Cell Biology, SUNY Downstate Medical Center, Brooklyn, NY, USA

<sup>2</sup> Center for Neural Science, NYU, New York, NY, USA

\*ads420@nyu.edu

## Abstract

Brain function is based on communication between individual cells, neurons and glia. From a traditional point of view, neurons play a central role in the fast transfer of information in the central nervous system while astrocytes, major type of glia, serve as housekeeping elements maintaining homeostasis of the extracellular microenvironment. This view has dramatically changed in recent years as many findings ascribe new roles to astrocytes. It is becoming evident that astrocytes communicate with neurons via chemical signals released to the extracellular space (ECS). Astrocytes also have communication systems of their own, such as calcium waves that use gap junctions in combination with purinergic signaling through the ECS. Here we discuss yet another important role for astrocytes: that they regulate diffusion of signaling molecules and therapeutic agents in the extracellular microenvironment by contributing to the structural properties of ECS. There is a wealth of morphological data showing that each astrocyte is an exclusive occupant of a small volume of brain tissue, and that many fine astrocytic processes ensheath neuronal processes and bodies. The functional significance of these unique morphological features is largely unknown with the exception of astrocytic coverage of synaptic formations. At the synapses, astrocytic processes play an active role by restricting neurotransmitter diffusion to the synaptic cleft and its immediate vicinity. Recent work suggests that astrocytic processes work in a similar fashion throughout the ECS and thus control the diffusive spread of substances over both short and long distances.

## Keywords

Brain, astrocyte, extracellular space, diffusion, tortuosity, volume fraction, dead spaces, aquaporin, ischemia, glioma

## 1. Introduction

Astrocytes are a major type of glial cell in the central nervous system (CNS). They maintain homeostatic levels of extracellular ions, pH, and express a variety of channels and transporters, most notably potassium channels, water channel aquaporin-4 (AQP4) and glutamate transporters. A wealth of new data suggests that astrocytes should not be viewed as passive elements. Indeed, astrocytes form a distinct network where individual cells interconnected via gap junctions propagate calcium waves and they also release a number of neuroactive substances to signal to neurons and to modulate neuronal transmission.

To fulfill such diverse functions, astrocytes need to be uniformly distributed throughout the neuropil in order to sustain their homeostatic functions, but at the same time their processes need to be present at specific locations within the neuropil (e.g. close to the neuronal synapses) in order to actively modulate synaptic transmission. This is accomplished through a particular distribution of astrocytes within the underlying neuropil and through complex geometry of astrocytic processes. It has been reported that each astrocyte occupies a separate anatomical domain resulting in a non-overlapping tiled layout [1, 2, 3] in the neuropil. It has also been



shown that astrocyte morphology is very complex. Specifically, fine astrocyte processes, which account for about 85% of astrocyte volume [1], wrap neuronal synapses and insert themselves between the dendrites and somata of neurons [4, 5, 6].

Here we discuss yet another important role for astrocytes: that they regulate extracellular diffusion by contributing to the structural properties of the ECS. Brain ECS surrounds individual cells in the CNS. It facilitates the diffusion-mediated transport of ions, neurotransmitters, metabolites, and it is also the final route for drug delivery to the brain cells. The distribution of substance in the ECS is regulated by the two macroscopic parameters of ECS – tortuosity and volume fraction [7]. This review will focus on the contribution of astrocytes to diffusion hindrance in brain ECS and extracellular volume regulation during physiological and pathological conditions.

## 2. Brain extracellular space

The ECS can be imagined as a system of contiguous narrow spaces demarcated by cellular membranes (Figure 1). The geometry of the ECS is defined by the shape of brain cells and the width of the pores between the cells. The ECS is filled with ionic solution and macromolecules of the extracellular matrix (ECM), predominantly proteoglycans and glycosaminoglycans. The width of individual interstitial spaces in the live brain tissue is estimated at 30-60 nm [8, 9]. The ECS serves as an important functional counterpart of neuronal and glia networks; it facilitates diffusion of neurotransmitters, neuromodulators, nutrients, metabolites, and therapeutic agents.

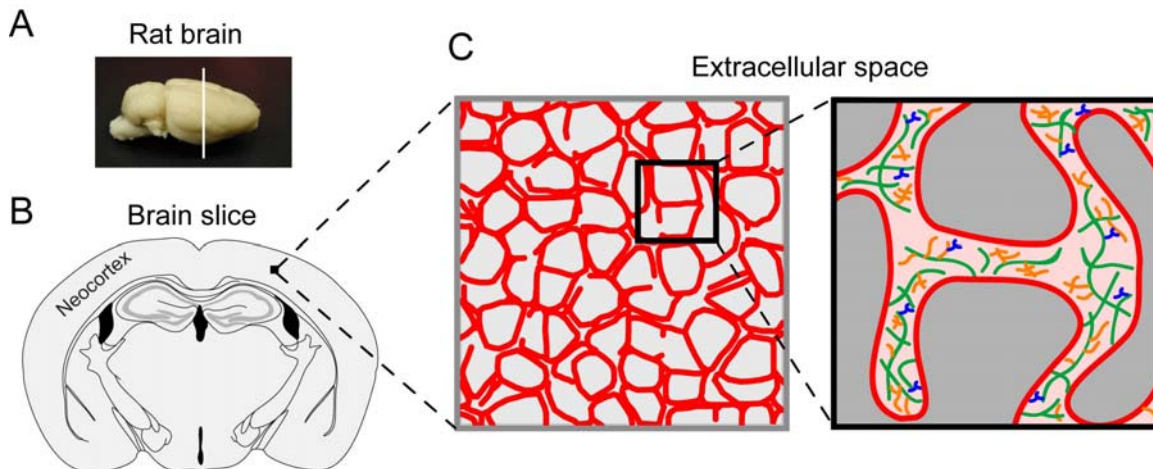


Figure 1. Brain extracellular space. A. Photograph of a rat brain. White line shows a plane of cutting for coronal brain slices. B. Schematic of a coronal brain slice. Diffusion studies are often carried out in the neocortex (labeled). C. Left: Schematic of microscopic architecture; cells are gray, ECS is red. Right: The ECS is filled with ionic solution and macromolecules of extracellular matrix (green, orange and blue).

Diffusion can be exploited experimentally to quantify macroscopic properties of the ECS in a live brain tissue. Diffusion experiments employing small extracellular probe molecules quantify two parameters of the ECS structure: the volume fraction and the tortuosity. The volume fraction ( $\alpha$ ) represents the proportion of tissue volume occupied by the ECS. The tortuosity ( $\lambda$ ) quantifies the hindrance imposed on the diffusion process by the tissue relative to an obstacle-free medium. Tortuosity is defined as  $(D/D^*)^{1/2}$ , where  $D$  and  $D^*$  are the free diffusion coefficient in a free medium and effective diffusion coefficients in brain, respectively [10, 7]. Alternatively, diffusion hindrance can be also defined as diffusion permeability ( $\theta$ ), which is a ratio of the effective diffusion coefficient in the brain tissue and the free diffusion coefficient [11]. In

isotropic healthy brain,  $\alpha$  is about 0.2 (i.e., about 20% of brain tissue volume resides in the ECS) and  $\lambda$  is about 1.6 (i.e., diffusion of a small extracellular probe molecule in brain tissue is slowed down about 2.5 times) [7, 12].

The structure of brain ECS dynamically changes during various physiological conditions such as neuronal activation and osmotic challenge [13, 12]. Recent study from Nedergaard's group [14] put ECS research in the limelight when it reported that  $\alpha$  constricts during an awake state and widens during the sleep state, and that the enlargement during sleep is necessary for removal of toxins and metabolites from brain tissue. The ECS structure also changes, often permanently, during pathological conditions, brain trauma and disease. For example, diffusion is significantly hindered and the volume of the ECS is reduced in many neuropathological states associated with cellular edema [13, 15, 16]. Among the many consequences of the impaired transport is the disruption of nutrient and metabolic trafficking, which augments brain dysfunction and prevents recovery.

### 3. Methods to study extracellular space

Many fundamental studies exploring ECS structure [12] utilized the diffusion-based Real-Time Iontophoretic (RTI) method [10]. The original study [10] employed four different small extracellular probe molecules, two cations and two anions, to measure  $\alpha$  and  $\lambda$  in rat cerebellum *in vivo*. Because all four ions gave very similar results, later studies predominantly employed tetramethylammonium ( $\text{TMA}^+$ ,  $MW$  74) for its relative ease of use, and the RTI method was called the TMA method in some studies.

The RTI method (Figure 2) uses the distribution of extracellular probe molecules released from a point source to quantify the aggregate parameters of the ECS,  $\alpha$  and  $\lambda$ , from a large region, typically containing hundreds of cells. In the RTI method, charged extracellular probe molecules are iontophoretically-delivered from a micropipette, and they are detected by an ion-selective microelectrode (ISM) positioned about 100-200  $\mu\text{m}$  away from the source. Concentration profiles recorded at the ISM are analyzed using the appropriate solution of the diffusion equation [7, 17].

In its early days, results obtained with the RTI method had been compared with the values of ECS parameters obtained by different methods, specifically radiotracer and morphometric methods. The radiotracer method pioneered by groups around Fenstermacher and Patlak [18, 19] utilized radioactive sucrose or inulin which were delivered into the ventricle and their distributions were obtained postmortem from sections of the caudate nucleus, the region adjacent to ventricles. The parameters measured in several species were in the range 15-20% for  $\alpha$  and 1.52-1.64 for  $\lambda$  [20]. Results obtained with the RTI and the radiotracer methods were in a good agreement.

The morphometric method relies on electron micrographs, which directly visualize the interstitial channels in a small region of fixed tissue, typically containing a few cells. Unfortunately, conventional fixation procedures cause water redistribution and they significantly distort ECS parameters [21, 8, 9, 22]. Studies employing freeze substitution, which to some extent remedies the shortcomings of conventional fixation, arrived at values of  $\alpha$  ranging from 0.15 to 0.20 [21], closer to the values typically obtained with diffusion methods [20, 23].

Diffusion method RTI offers two important advantages over the morphometric method. It yields both  $\alpha$  and  $\lambda$ , while the morphometric method quantifies only  $\alpha$ . In addition, the RTI can be used in live tissue and thus can be exploited to study dynamic changes of the ECS during various physiological and pathological conditions [23, 13, 7, 12, 14, 24, 25]. It is beyond the scope of this review to provide further details on diffusion methods and their theoretical underpinning. We refer reader to published articles and reviews on this topic [10, 7, 17, 26].

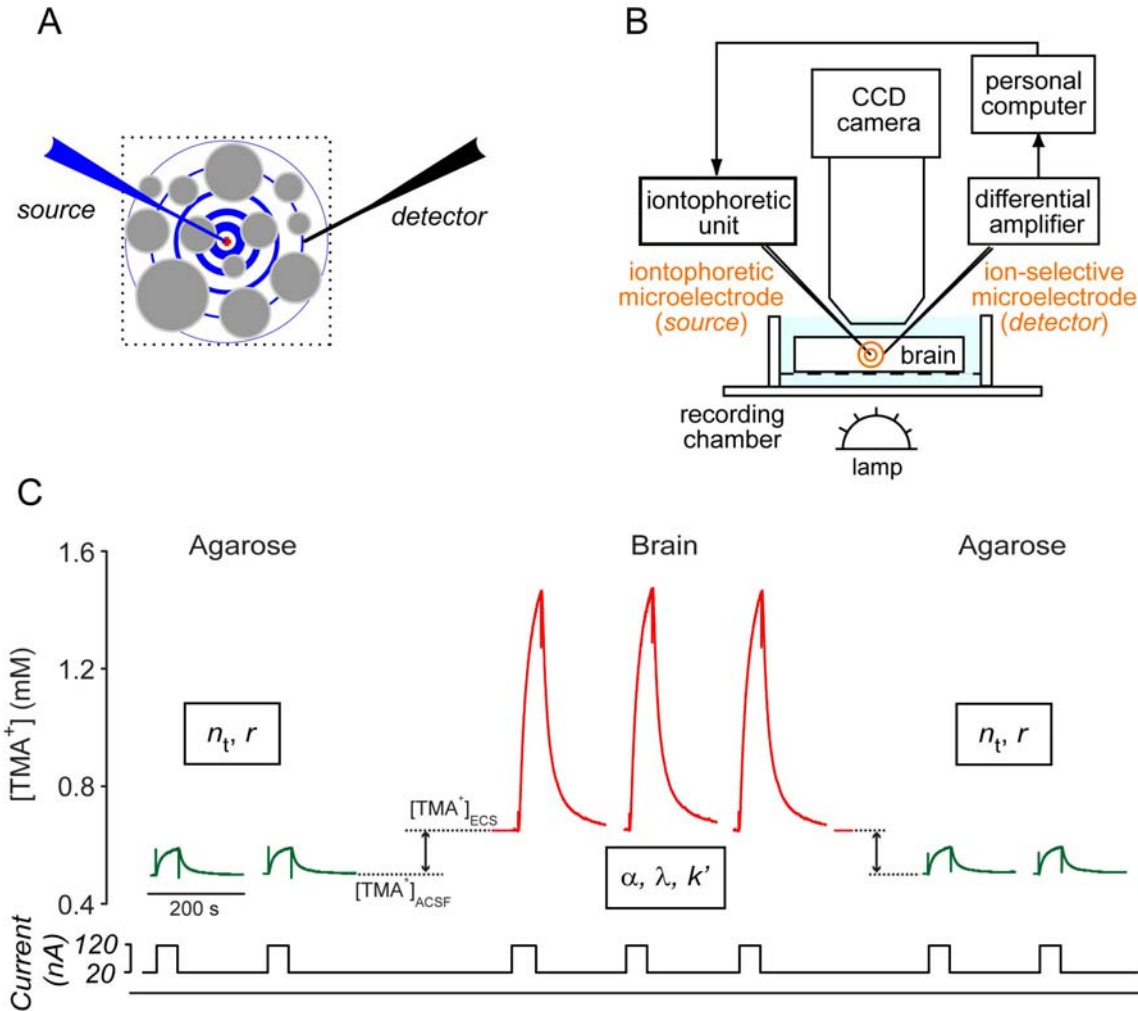


Figure 2. Real-Time Iontophoretic method. A. Point source is used to release extracellular marker molecule. Detector could be another micropipette (as shown here) or a CCD camera when fluorescently labeled marker molecules are used (as in Integrative Optical Imaging method [67], not shown). B. Setup used for RTI measurements. C. A typical time line of an RTI experiment. Diffusion measurements in brain tissue are preceded and followed up by diffusion measurement in dilute agarose to determine transport number of iontophoretic microelectrode ( $n_t$ ) and a spacing between the ion-selective microelectrode and the iontophoretic microelectrode ( $r$ ). Measurements in brain tissue quantify  $\alpha$ ,  $\lambda$ , and a non-specific clearance  $k'$  ( $s^{-1}$ ) [17]. (Modified from [68])

#### 4. Astrocytes

Astrocytes (Figure 3) are one type of glial cell that are the most plentiful of the brain cells in the central nervous system. The other glial cells are microglia and oligodendrocytes. Astrocytes have a small cell body with a few major processes containing the intermediate protein glial fibrillary acidic proteins (GFAP). The major processes extend into morphologically complex fine processes devoid of GFAP. The thin and thread-like fine processes, which account for about 85% of an astrocyte's volume and insert themselves between the dendrites and somata of neurons, line the pia mater as glial limitans, and form glial end-feet on blood vessels [5, 6]. Each individual

astrocyte establishes its own exclusive microdomain by avoiding interdigitations with processes from neighboring astrocytes, while ensheathing numerous dendrites and somas in the neuropile [1, 2, 3]. This arrangement allows astrocytes to function as a diffusion barrier for the signaling molecules and ions released in the ECS synaptically and extrasynaptically, thereby contributing to the structural properties of ECS.

Astrocytes take part in various functions that are important for normal functioning of neurons. Astrocytes have the major  $\text{Na}^+$ -dependent glutamate transporter GLUT-1 and GLAST that removes the excess glutamate released during synaptic transmission. Once accumulated inside astrocytes, glutamate is converted to glutamine with the enzyme glutamine synthetase and transported back to neurons. Astrocytes are also involved in the homeostasis of extracellular potassium. During neuronal activity, the extracellular concentration of potassium increases from 5 to 10-12 mM. Astrocytes remove excess potassium through a passive mechanism called “spatial buffering” facilitated by inward rectifier  $\text{K}^+$  channels, and through a  $\text{Na}^+/\text{K}^+$ -ATPase pump that pumps  $\text{K}^+$  along with water molecules inside astrocytes [27]. The plasticity of morphology of astrocytes can be induced by neuronal activity and neuromodulators, and depending on the signal, the fine astrocytic processes may retract or extend in the neuropil [27, 28].

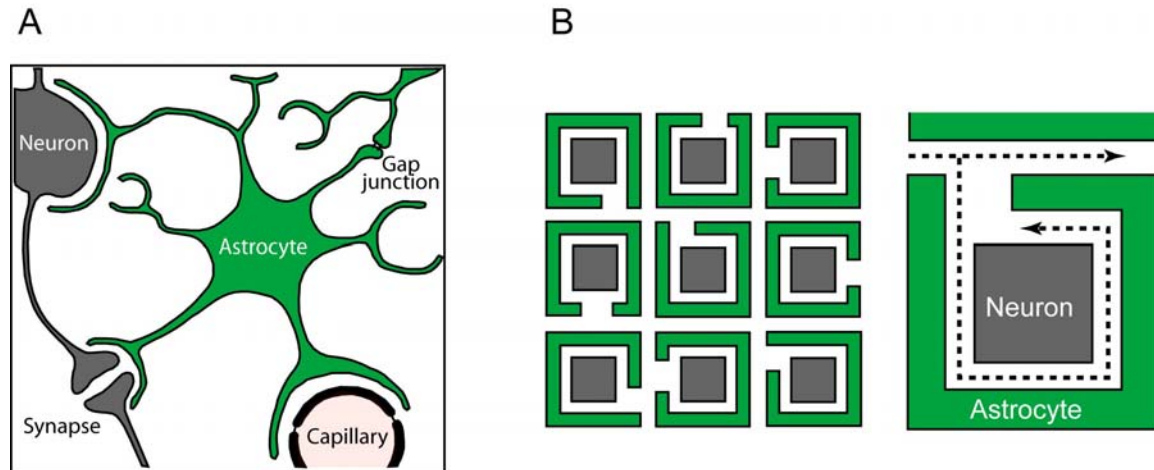


Figure 3. Astrocytes in brain tissue. A. Astrocytes have a small cell body with a few major proximal processes. About 85% of astrocyte volume resides in fine distal processes [1], which wrap around neuronal cell bodies, synapses and form end feet on blood vessels. Astrocytes are connected with each other by membrane adhesions called gap junctions. B. Concave astrocytic wrappings were proposed to form dead space microdomains in brain ECS [58].

## 5. Astrocytes and extracellular space under physiological conditions

Values of ECS parameters reviewed in this section are summarized in Table 1.

### 5.1. ECS in a sleep-wake cycle

The ECS occupies about 20% of the total tissue volume ( $\alpha \sim 0.20$ ) and the tortuosity is about 1.6. Recent work from Maiken Nedergaard’s group suggested that the traditionally reported value of  $\alpha$  corresponds to the ECS volume during a sleep state, and that during an awake state, the ECS volume dramatically decreases [14]. The study utilized the RTI method in the cortex of mice during naturally occurring sleep, when awake and during anesthesia. For RTI measurements performed in sleeping animals at midday, the value of  $\alpha$  averaged at 0.234 but when the RTI records were taken in awake animals in the evening,  $\alpha$  was only about 0.141. A similar result was

obtained when the sleep state was induced pharmacologically:  $\alpha = 0.136$  increased to 0.227 after animals were anesthetized with a ketamine-xylazine mixture. Interestingly, values of tortuosity remained similar in these two brain states.

The study by Xie and co-workers [14] has fundamental implications for brain function and it raises many interesting questions. As the ECS volume transitions from the sleep state to the awake state and back, volume of some other compartment or compartments must cycle in a reciprocal manner. Maintenance of a reduced ECS volume in the awake state appears to be driven by noradrenergic afferents, diffusely innervating the neocortex, which is known to cause wakefulness and vigilance [29, 30]. Xie and co-workers [14] reported that a cocktail of adrenergic antagonists applied on the cortical surface of an awake animal increased ECS volume from 0.143 to 0.226, implicating the adrenergic system in reversal of the ECS volume fraction from the “awake” state to the “sleep” state. It remains to be determined which compartment is involved in the ECS volume changes during the sleep-wake cycle. Astrocytes are one of the possible candidates because they are well-suited for water uptake and transport and they express adrenergic receptors [31].

## **5.2. Structural plasticity of astrocytes during lactation and dehydration**

There is a wealth of evidence to suggest that the ECS is a dynamic structure and that its properties change during various physiological and pathological conditions [23, 13]. Is there also evidence for dynamic changes of astrocyte shape and volume under physiological conditions? Indeed, there is a classic example where structural plasticity of astrocytes occurs physiologically. In the hypothalamo-neurohypophysial system, cellular architecture undergoes remarkable reversible structural changes in dehydration [32, 33] and lactation [34]. Astrocytic processes play a primary role in this phenomenon.

In the supraoptic nucleus of hypothalamo-neurohypophysial system, astrocytes form a thin layer called the ventral glial zone that lies between the magnocellular neurons and pia mater. Some processes of these astrocytes extend to the somatodendritic zone where they cover soma and dendrites of magnocellular neurons in the basal state. During dehydration or lactation, the astrocytic processes retract from the somatodendritic zone while somata of magnocellular neurons enlarge and form neuron-neuron appositions [35, 36]. Functionally, the withdrawal is interpreted as a removal of diffusion barriers from the somatodendritic zone, which in turn enhances the excitation of neurons and thus hormonal release from axon terminals of magnocellular neurons located in the neurohypophysis [35, 36].

This interpretation was tested in a study combining electrophysiology with diffusion analysis in rat hypothalamic slices from virgin and lactating female rats [37]. These workers found that synaptic crosstalk was enhanced in the somatodendritic zone of the supraoptic nuclei from lactating female rats. Using diffusion analysis, they reported significant changes in the ECS structure in lactating animals. In the somatodendritic zone of virgin rats, extracellular diffusion of TMA was anisotropic ( $\lambda_x = 1.39$ ,  $\lambda_y = 1.48$  and  $\lambda_z = 1.50$ ) and  $\alpha$  was 0.32. During lactation when astrocytic processes retracted from the somatodendritic zone, extracellular diffusion of TMA was less hindered and isotropic ( $\lambda_x = 1.34$ ,  $\lambda_y = 1.39$  and  $\lambda_z = 1.36$ ) while ECS volume significantly decreased to a value of 0.20. In summary, withdrawal of astrocytic processes led to a removal of some diffusion barriers, which was detected as a decrease of extracellular hindrance to diffusion, while the decrease in ECS volume is likely attributed to enlargement of neuronal cell bodies.

## **5.3. Role of AQP4 and alpha-syntrophin in ECS volume maintenance**

Values of  $\alpha$  and  $\lambda$  are fairly constant among different brain regions but they reversibly change during neuronal activity [12] and one wonders how the ECS volume and tortuosity are maintained

and regulated. Studies in AQP4-deficient mice and alpha-syntrophin-deficient mice brought some answers to these questions.

Astrocytes express aquaporin-4 (AQP4) water channels. These channels are predominantly expressed on the membranes of astrocytic endfeet facing perivascular spaces and on glia limitans adjacent to the sub-arachnoid spaces, but they are also expressed on the astrocytic membranes in the neuropil [38, 39]. The function of AQP4 channels was studied in transgenic mice where the AQP4 gene was knocked-out. It was shown that the expression of AQP4 channels on the astrocytic membranes was significantly reduced in AQP4 knock out mice [40] and it was proposed that water compartmentalization might be altered.

**Table 1.** ECS parameters measured with RTI method under physiological conditions and during genetic manipulations.

Condition	Region	Species	Prep	$\alpha$	$\lambda$	Ref #
Sleep	Cortex	Mouse	<i>in vivo</i>	0.23	1.3-1.8	14
Awake	Cortex	Mouse	<i>in vivo</i>	0.14	1.3-1.8	14
Virgin	Supraoptic nucleus	Rat	slice	0.32	(1.39,1.48,1.50) <sup>1</sup>	37
Lactation	Supraoptic nucleus	Rat	slice	0.20	(1.34,1.39,1.36) <sup>1</sup>	37
AQP4+/+	Somatosensory cortex	Mouse	<i>in vivo</i>	0.18	1.61	41
AQP4-/-	Somatosensory cortex	Mouse	<i>in vivo</i>	0.23	1.62	41
AQP4+/+	Somatosensory cortex	Mouse	<i>in vitro</i>	0.19	1.61	41
AQP4-/-	Somatosensory cortex	Mouse	<i>in vitro</i>	0.23	1.64	41
$\alpha$ -syn+/+	Cortex	Mouse	<i>in vivo</i>	0.20	1.60	43
$\alpha$ -syn-/-	Cortex	Mouse	<i>in vivo</i>	0.23	1.60	43
$\alpha$ -syn+/+	Cortex	Mouse	<i>in vitro</i>	0.19	1.50	43
$\alpha$ -syn-/-	Cortex	Mouse	<i>in vitro</i>	0.21	1.50	43

<sup>1</sup>Anisotropy tensor ( $\lambda_x, \lambda_y, \lambda_z$ ), AQP4: aquaporin 4,  $\alpha$ -syn: alpha-syntrophin. (Modified from [12])

Yao and co-workers [41] showed that ECS volume was significantly larger in the somatosensory neocortex of AQP4-deficient mice. In WT mice, ECS volume was 0.18 and 0.19 in *in vivo* preparation and *in vitro* preparation, respectively, but it increased by about 25% (to 0.23) in the AQP4-deficient mice. There were no significant differences in  $\lambda$  values measured in these two genotypes suggesting the extracellular hindrance for small ions remains unaltered. Study by Yao and co-workers [41] provided direct evidence for the role of AQP4 channels in



homeostasis of the ECS volume fraction, and it was argued that enlarged ECS volume may account for lower susceptibility of AQP4 mice to seizure [42] either because of lower accumulation of potassium or because of reduced ephaptic interactions in the enlarged ECS of AQP4-deficient mice.

Findings of Yao and co-workers [41] in AQP4-deficient mice were further supported by a study in alpha-syntrophin-deficient mice [43]. Alpha-syntrophin ( $\alpha$ -syn) is an intracellular adapter protein which anchors AQP4 channels in specific areas of astrocytic membrane. Deletion of alpha-syntrophin reduces the amount of AQP4 in perivascular and subpial membranes, although the total AQP4 protein content in the brain remains constant. Using RTI method, Dmytrenko and co-workers [43] reported an enlargement of the ECS volume but no change in the tortuosity in *in vivo* and *in vitro* neocortex of the alpha-syntrophin-deficient mice. In WT mice, ECS volume was 0.20 and 0.19 in *in vivo* preparation and *in vitro* preparation, respectively, but it increased to 0.23 and 0.21 in *in vivo* preparation and *in vitro* preparation, respectively, in the alpha-syntrophin-deficient mice.

Taken together, studies in AQP4- and alpha-syntrophin-deficient mice revealed that astrocytes participate in water compartmentalization in brain tissue for under resting conditions. Furthermore, AQP4 and alpha-syntrophin contribute to capacity for water transport across astrocytic membranes during a reversible challenge.

## 6. Astrocytes and extracellular spaces under pathological conditions

Values of ECS parameters reviewed in this section are summarized in Table 2.

### 6.1. Response of astrocytes and ECS to ischemic conditions and osmotic stress

Astrocytes are the major cell type to swell and to exhibit reactive astrogliosis under many pathological conditions, such as ischemia, traumatic brain injury, hepatic encephalopathy, hyponatremia, and status epilepticus [44, 45, 46]. Cellular edema accompanies various brain diseases, and it occurs when water moves from the ECS into the brain cells. Various mechanisms of astrocytic swelling have been proposed. Most notably, intracellular accumulation of electrolytes and uptake of glutamate are believed to cause astrocytic swelling in ischemia and traumatic brain injury [46]. The pathological consequences of astrocyte swelling include compression of blood vessels, release of excitatory amino acids, activation of volume-dependent anion channels, and alteration in the structural parameters of ECS [46, 12].

Structural parameters of ECS have been studied *in vitro* and *in vivo* in pathologies accompanied by cell swelling. Generally,  $\lambda$  increases and  $\alpha$  decreases in an *in vitro* model of ischemia and during anoxia *in vivo* [23]. Rice and Nicholson [47] measured  $\lambda$  and  $\alpha$  during hypoxia mimicked by superfusing rat striatal slices with the ACSF containing 95% N<sub>2</sub>-5% CO<sub>2</sub> for 10-30 minutes. They found no significant change in  $\lambda$ , but saw a significant decrease in  $\alpha$  from 0.21 to 0.13. Later, Perez-Pinzon and co-workers [48] induced an *in vitro* ischemic condition for 10-30 minutes in rat brain slices by oxygen-glucose deprivation that included maintaining the same anoxic condition above the slice. ECS parameters were measured in the stratum pyramidale of CA1 and CA3 hippocampal region and neocortex. The control values of  $\lambda$  were 1.50, 1.57, and 1.62 and  $\alpha$  were 0.14, 0.20, and 0.18 in CA1, CA3, and cortex, respectively. During anoxic depolarization,  $\alpha$  decreased to 0.05, 0.13, and 0.09 in CA1, CA3, and cortex, respectively. The only significant change in  $\lambda$  occurred in CA3, where it increased to 1.73 during anoxic depolarization. Significant changes in the ECS parameters were also reported in the study employing an *in vitro* thick-slice (1000  $\mu$ m) model of ischemia [49]. This preparation is a better approximation of the *in vivo* ischemia because the clearance of ions and neurotransmitters to the ACSF superfusing the tissue is hindered by the slice thickness, in addition to depriving the tissue



of oxygen and glucose. Hrabetova and Nicholson [50] reported  $\lambda = 1.99$  and  $\alpha = 0.12$  in the rat neocortex of 1000  $\mu\text{m}$  slices.

ECS parameters were also studied during ischemia and terminal anoxia *in vivo*. Sykova and co-workers [51] measured  $[\text{K}^+]_{\text{ECS}}$ ,  $\lambda$ , and  $\alpha$  *in vivo* in the dorsal horn of rat spinal cord during progressive ischemia induced by exsanguinations, and terminal anoxia induced either by respiratory arrest or by cardiac arrest. During progressive ischemia the blood pressure fell to 50-60 mm Hg,  $[\text{K}^+]_{\text{ECS}}$  increased to 6-12 mM,  $\lambda$  remained constant but  $\alpha$  decreased from 0.20 to 0.16. During severe ischemia when the blood pressure fell to 20-30 mm Hg,  $[\text{K}^+]_{\text{ECS}}$  increased to 60-70 mM,  $\lambda$  increased to 2.00 and  $\alpha$  decreased to 0.05. Similar results were obtained by Vorisek and Sykova [52] during *in vivo* ischemia in rat neocortex and corpus callosum where  $\lambda$  increased to 2.00-2.10 while  $\alpha$  decreased to 0.05-0.06. It is interesting to note that even in the most extreme conditions of cellular swelling, such as during terminal anoxia, the ECS never becomes completely obliterated. This might be due to presence of the ECM, which keeps the interstitial spaces accessible even in the most extreme conditions.

## 6.2. Dead space hypothesis

Diffusion studies discussed above show that the structural parameters of the ECS change dramatically in pathologies accompanied by cell swelling. How can we interpret these findings? It is plausible that during these pathologies, brain cells swell and the ECS volume decreases as water shifts between these two compartments. It has been hypothesized that the swelling of brain cells creates dead space (DS) microdomains in the ECS that transiently trap diffusing molecules and slow down their travel through the ECS thereby increasing the tortuosity [16] (Figure 4). Electron micrographs obtained from ischemic neocortex show occlusion of the gaps between cells [53]; such dead-end pores may form the DS microdomains. It has been also shown that when macromolecules, such as 70 kDa dextran, were applied to the ischemic tissue,  $\lambda$  decreased from 2.00 to 1.54 and  $\alpha$  decreased from 0.12 to 0.10 [50]. It had been hypothesized that dextran macromolecules eliminated the DS microdomains by occluding them. Hrabetova and co-workers [16] went on to show that an apparent diffusion coefficient of 70 kDa dextran in ischemic tissue decreases over time, which was consistent with the idea that 70 kDa dextran gets trapped in the DS microdomains. Taken together, cell swelling and changes in cell shape correlate with profound changes in the ECS parameters during ischemic conditions and these findings can be explained by DS hypothesis.

Simulation and theoretical work have also provided support for the DS hypothesis (Figure 4). Researchers have used MCell (Monte Carlo Simulator of Cellular Microphysiology) software [54] to simulate diffusion in virtual models of ECS and to test how geometry of cell contributes to  $\lambda$ . Theoretical work and simulations of diffusion in model media composed of convex cellular elements revealed an upper limit of 1.225 for  $\lambda$  [55, 16, 56, 11]. This value of  $\lambda$  is significantly lower than the hindrance measured in the brain under control conditions (about 1.6) and during ischemia (about 2.0). The DS hypothesis proposed that a more complex geometry of ECS containing dead-end pores or voids could explain  $\lambda$  measured in brain tissue [16, 11]. Mathematical modeling studies supported prediction of the DS microdomain hypothesis when simulations showed that  $\lambda$  increased to and above the values typically measured in brain when the DS microdomains are modeled as dead-end pores or voids [11, 57].

## 6.3. ECS parameters during astrocyte-selective manipulation

Because of morphological complexity, astrocytic fine processes were proposed to be implicated in the formation of dead-space microdomains [11, 58, 16] (Figure 3). To further test this idea, Sherpa and co-workers [25] applied a gliotoxin DL- $\alpha$ -Aminoadipic Acid (DL-AA) to selectively and reversibly swell astrocytes in the somatosensory neocortex of rat brain slices and measured  $\lambda$  and  $\alpha$ . It was expected that swollen astrocytic processes would create additional dead spaces.

The authors reported that  $\lambda$  increased from 1.63 to 1.71 while  $\alpha$  decreased from 0.22 to 0.14 during DL-AA application. During recovery,  $\lambda$  remained elevated at 1.73 while  $\alpha$  recovered to a control value of 0.20. Persistent increase in  $\lambda$  during the application of DL-AA and during the recovery suggested that the geometry of astrocytic processes was altered as the astrocytes swelled in DL-AA, and that this modified geometry of astrocytic processes persisted even during the recovery when shrinking astrocytic processes recovered the ECS volume. These observations led authors to conclude that the increased extracellular hindrance to diffusion was mediated via formation of additional dead-spaces in the ECS by astrocytic processes (Figure 5).

AQP4, a major water channel in the brain, is exclusive to astrocytes and it is anchored in the astrocytic end-feet and subpial surface. Because no physiologically compatible blockers of AQP4 are currently available, function of AQP4 in the neuropil is studied in transgenic animals

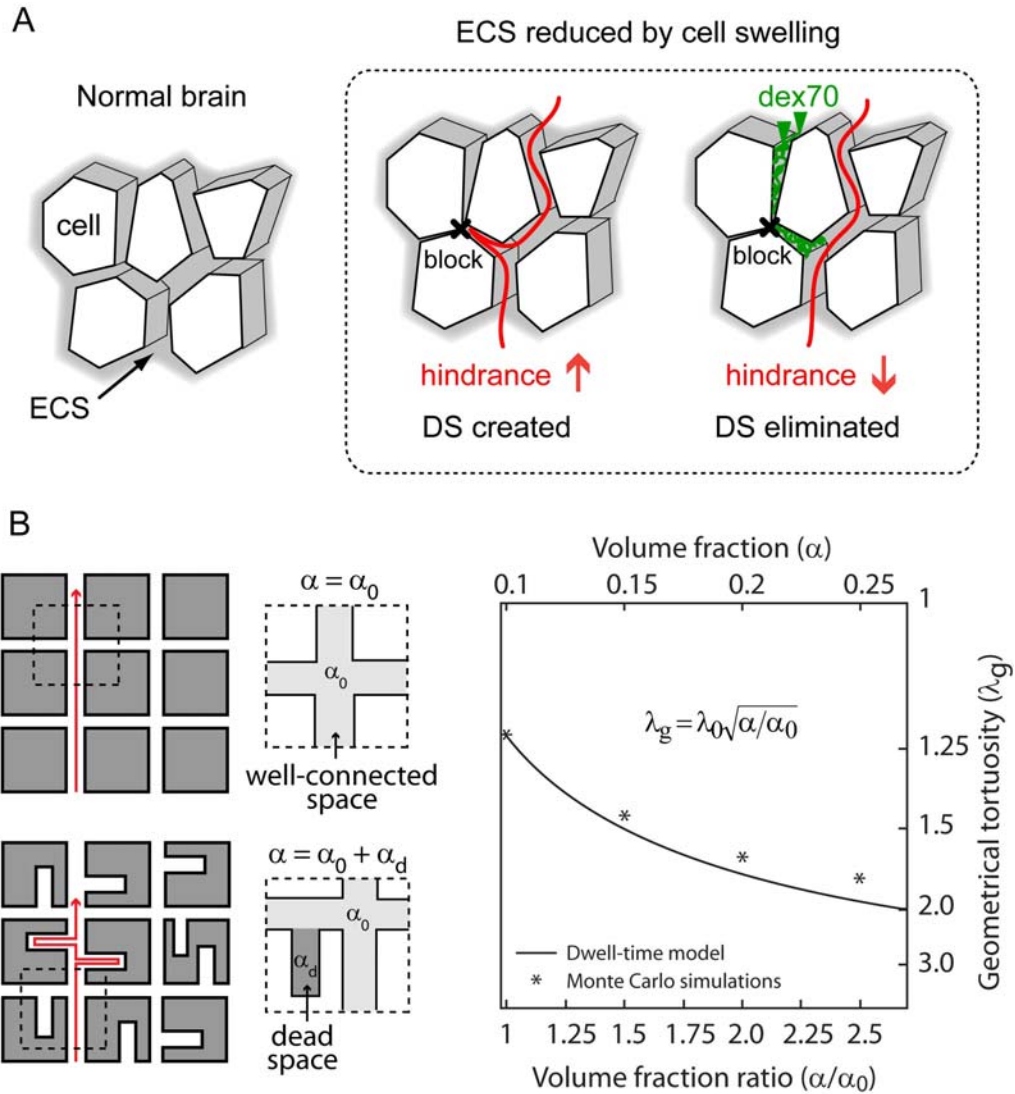


Figure 4. Dead space hypothesis. A. Extracellular diffusion during ischemia hindered by dead space microdomains. B. Dwell-time diffusion model in tandem with Monte Carlo simulations of diffusion [16, 11] show that dead spaces hypothesis can explain extracellular hindrance observed in brain under control conditions and in disease associate with cell swelling, such as ischemia. (Modified from [16, 17])

where AQP4 or its anchoring adapter protein alpha-syntrophin is removed. Deletion of AQP4 channels was shown to reduce astrocytic swelling and brain edema in water-intoxicated mice, ischemic stroke and transient focal cerebral ischemia [59, 60], suggesting its important role in water movement. Dmytrenko and co-workers [43] studied the impact of alpha-syntrophin deletion on ECS parameters in the cortex of mice during hypotonic stress and elevated potassium *in vitro*, and during severe pathological conditions *in vivo*. During exposure of brain slices to a severe form of hypotonic stress (-100 mOsmol/L) and an elevated level of extracellular  $K^+$  (10 mM; normal is 3-5 mM), a significant but small decrease in  $\alpha$  was observed in the alpha-syntrophin-deficient mice compared to the wild-type mice; a mild form of hypotonic stress (-50 mOsmol/L) was ineffective in changing  $\alpha$ . Severe forms of pathological condition such as terminal anoxia/ischemia led to a smaller decrease in  $\alpha$  in the alpha-syntrophin-deficient mice (0.14) compared to the wild-type mice (0.10) *in vivo* while  $\lambda$  attained a significantly high value of 2.25. In summary, Dmytrenko and co-workers [43] inferred that water transport through the AQP4 channel is more critical during pathological condition than during physiological condition.

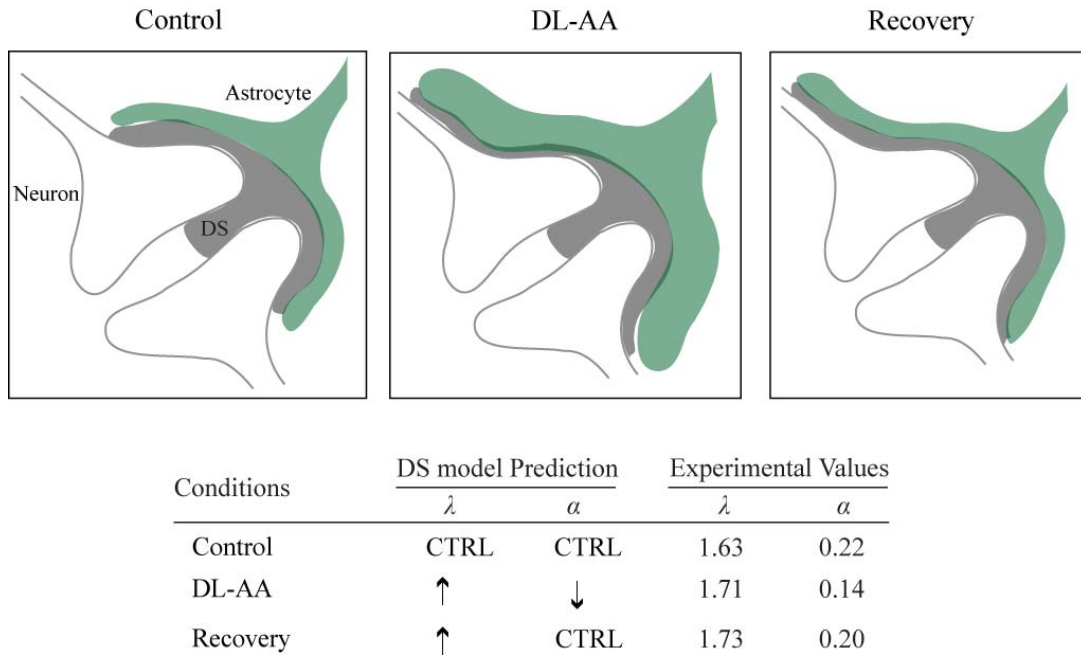


Figure 5. A schematic diagram showing that the DS hypothesis predicts the increase in extracellular hindrance seen during DL-AA application in rat somatosensory neocortex. (Modified from [25])

Taken together, multiple studies indicate that the ECS parameters are significantly altered during ischemic conditions and in anoxia [51, 50, 15]. Astrocytic swelling is a hallmark of these pathologies and it significantly contributes to the changes in ECS parameters. Altered  $\lambda$  and  $\alpha$  impair diffusion of metabolites, therapeutic agents, and affect neuron-neuron and neuron-glia communication. In addition, accumulation of potassium ions, excitatory amino acids such as glutamate, and acidosis in the reduced ECS volume is likely to intensify insult. AQP4 channels play a crucial role in maintenance of ECS volume and they mediate, in part, water redistribution during conditions mimicking intense neuronal activity, cell swelling and ischemic conditions.

**Table 2.** Values of ECS parameters measured with RTI method under pathological conditions.

<b>Pathology</b>	<b>Region</b>	<b>Species</b>	<b>Prep</b>	<b><math>\alpha</math></b>	<b><math>\lambda</math></b>	<b>Ref #</b>
Ischemia	Cortex	Rat	thick-slice	0.1-0.15	1.79-1.99	50,15,16
Ischemia	Cortex	Rat	slice	0.09	1.74	48
Ischemia	CA1	Rat	slice	0.05	1.73	48
Ischemia	CA3	Rat	slice	0.13	1.73	48
Hypoxia	Neostriatum	Rat	slice	0.13	1.53	47
Ischemia/Anoxia	Spinal cord, dh	Rat	<i>in vivo</i>	0.05	2.00	51
Ischemia	Cortex	Rat	<i>in vivo</i>	0.06	2.00	52
Ischemia	Corpus callosum	Rat	<i>in vivo</i>	0.05	2.10	52
Gliotoxin	Som. cortex	Rat	<i>in vitro</i>	0.14	1.71	25
Pilocytic Astrocyt. GR I	Cortex	Human	slice	0.37	1.50	62
Diffuse Astrocyt. GR II	Cortex	Human	slice	0.29	1.81	62
Anaplastic Astrocyt. GR III	Cortex	Human	slice	0.44	1.78	62
Glioblastoma GR IV	Cortex	Human	slice	0.58	1.35-1.83	62
Oligodendrogliomas GR II	Cortex	Human	slice	0.23	1.50	62
Ependymomas GR II	Cortex	Human	slice	0.39	1.55	62
Medulloblastomas	Cortex	Human	slice	0.38	1.57	62

dh: dorsal horn, Som: somatosensory,  $\alpha$ -syn: alpha-syntrophin, GR: Grade, Astrocyt: Astrocytomas. (Modified from [12])

#### 6.4. Gliomas

Gliomas are brain tumors that are derived from glial cells or their precursors. Malignancy grades of gliomas are graded according to neuropathological criteria developed by World Health Organization (WHO) [61]. Glioma cells proliferate and migrate through interaction with the ECM molecules, and this behavior of glioma cells could potentially be affected by the size and contents of the ECS [62]. Earlier electron microscopy studies [63] and radioactively labeled sucrose [64] suggested an enlarged ECS volume in human gliomas. Vargova and co-workers

[62] measured  $\lambda$  and  $\alpha$  in human brain tumors of various malignancy grades using the RTI method. The control group comprised of brain tissue samples from patients undergoing treatment for temporal lobe epilepsy.

Analysis of TMA<sup>+</sup> diffusion measurements in control slices from human temporal cortex (layers III and IV) revealed  $\lambda = 1.55$  and  $\alpha = 0.24$ . Tortuosity remained in a range 1.50 – 1.55, but volume fraction increased to 0.37 in pilocytic astrocytomas (WHO grade I) and 0.39 in ependymomas (WHO Grade II). Tortuosity and volume fraction were significantly higher in diffuse fibrillary astrocytomas (WHO grade II) and they further increased in anaplastic astrocytoma (WHO grade III), where  $\lambda = 1.78$  and  $\alpha = 0.44$ . In glioblastoma (WHO grade IV),  $\alpha$  was 0.58 while  $\lambda$  ranged from 1.35 to 1.83. Measurements in oligodendrogliomas (WHO grade II) showed that  $\lambda = 1.50$  and  $\alpha = 0.23$ , similar to the control values. Medulloblastomas revealed a high  $\alpha$  (0.38) and a constant  $\lambda$  (1.57). Taken together, the authors found that ECS volume increases in all gliomas except oligodendrogliomas. In addition, the authors also investigated the relationship between ECS parameters of gliomas and their proliferative activity, and they found a positive correlation.

There was a significant increase in  $\lambda$  along with an increase in  $\alpha$ , especially in high-grade gliomas (III and IV). Such an increase in  $\lambda$  in high-grade glioma tissues was thought to be a consequence of remodeling of the ECM composition through overproduction of tenascin-R [65]. Increased hindrance to diffusion in gliomas presents a challenge for the diffusion of therapeutic agents. Therefore, studies of ECS parameters are not only important for understanding migratory behavior of glioma cells through an enlarged ECS but also for designing effective strategies for delivering therapeutic agents [66].

## 7. Conclusions

Brain ECS serves as an import functional counterpart of neuronal and glia networks, and it facilitates diffusion of neurotransmitters, neuromodulators, nutrients, metabolites and therapeutic agents. Recent studies suggest that astrocytes play a significant role in regulating macroscopic parameters of brain extracellular space. Using diffusion analysis as an experimental tool in these studies, researchers characterized the ECS structure under physiological conditions, and they also used models of neurological diseases to study how it changes during pathological conditions. This work has demonstrated that astrocytes contribute to diffusion hindrance in brain extracellular space and that they are also involved in the regulation of brain extracellular space volume under resting conditions and during brain activity. Moreover, the ECS structure was found to change, often dramatically and permanently, during pathological conditions, brain trauma and disease. These novel findings have important implications for physiology of the CNS, drug delivery strategies, and they significantly contribute to understanding the mechanisms and progression of multiple neurological and mental disorders.

## Acknowledgment

The authors are grateful to Robert Colbourn for critical reading of the manuscript. This work was supported by National Institute Of Neurological Disorders And Stroke of the National Institutes of Health under Award Number R01 NS047557.

## References

- [1] E. A. Bushong, M. E. Martone, Y. Z. Jones, M. H. Ellisman: *Protoplasmic astrocytes in CA1 stratum radiatum occupy separate anatomical domains*. J Neurosci **22**, 183-192 (2002)

- [2] K. Ogata, T. Kosaka: *Structural and quantitative analysis of astrocytes in the mouse hippocampus*. Neuroscience **113**, 221-233 (2002)
- [3] M.M. Halassa, T. Fellin, H. Takano, J. H. Dong, P.G. Haydon: *Synaptic islands defined by the territory of a single astrocyte*. J Neurosci **27**, 6473-6477 (2007)
- [4] J. Spacek: *Three-dimensional analysis of dendritic spines*. Anat Embryol **171**, 245-252 (1985)
- [5] T. Kosaka, K. Hama: *Three-dimensional structure of astrocytes in the rat dentate gyrus*. J Comp Neurol **249**, 242-260 (1986)
- [6] J. Grosche, V. Matyash, T. Möller, A. Verkhratsky, A. Reichenbach, H. Kettenmann: *Microdomains for neuron-glia interaction: parallel fiber signaling to Bergmann glial cells*. Nat Neurosci **2**, 139-143 (1999)
- [7] C. Nicholson: *Diffusion and related transport mechanisms in brain tissue*. Rep Prog Phys **64**, 815-884 (2001)
- [8] R. G. Thorne, C. Nicholson: *In vivo diffusion analysis with quantum dots and dextrans predicts the width of brain extracellular space*. PNAS **103**, 5567-5572 (2006)
- [9] F. Xiao, C. Nicholson, J. Hrabec, S. Hrabetova: *Diffusion of Flexible Random-Coil Dextran Polymers Measured in Anisotropic Brain Extracellular Space by Integrative Optical Imaging*. Biophys J. **95**, 1382-1392 (2008)
- [10] C. Nicholson, J. M. Philips: *Ion diffusion modified by tortuosity and volume fraction in the extracellular microenvironment of the rat cerebellum*. J Physiol **321**, 225-257 (1981)
- [11] J. Hrabec, S. Hrabetova, K. Segeth: *A model of effective diffusion and tortuosity in the extracellular space of the brain*. Biophys J **87**, 1606-1617 (2004)
- [12] E. Sykova, C. Nicholson: *Diffusion in brain extracellular space*. Physiol Rev **88**, 1277-1340 (2008)
- [13] E. Sykova, T. Mazel, L. Vargova, I. Vorisek, S. Prokopova-Kubinova: *Extracellular space diffusion and pathological states*. In: Progress in Brain Research. Vol 125, eds. Agnati LF, Fuxe K, Nicholson C, Sykova E, Elsevier Sciences, Amsterdam, pp. 155-178 (2000)
- [14] L. Xie, H. Kang, Q. Xu, M. J. Chen, Y. Liao, M. Thiyagarajan, J. O'Donnell, D. J. Christensen, C. Nicholson, J. J. Iliff, T. Takano, R. Deane, M. Nedergaard: *Sleep drives metabolic clearance from the adult brain*. Science **342**, 373-377 (2013)
- [15] S. Hrabetova, K. C. Chen, D. Masri, C. Nicholson: *Water compartmentalization and spread of ischemic injury in thick-slice ischemia model*. J Cereb Blood Flow Metab **22**, 80-88 (2002)
- [16] S. Hrabetova, J. Hrabec, C. Nicholson: *Dead-space microdomains hinder extracellular diffusion in rat neocortex during ischemia*. J Neurosci **23**, 8351-8359 (2003)
- [17] S. Hrabetova, Nicholson C: *Biophysical properties of brain extracellular space explored with ion-selective microelectrodes, integrative optical imaging and related techniques*. In: Electrochemical Methods for Neuroscience (Michael AC, Borland LM, eds), pp167-204. Florida: CRC (2007)
- [18] D. P. Rall, W. W. Oppelt, C. S. Patlak: *Extracellular space of brain as determined by diffusion of inulin from the ventricular system*. Life Sci **2**, 43-48 (1962)
- [19] V. A. Levin, J. D. Fenstermacher, C. S. Patlak: *Sucrose and inulin space measurements of cerebral cortex in four mammalian species*. Am J of Physiol **219**, 1528-1533 (1970)
- [20] J. D. Fenstermacher, T. Kae: *Drug 'diffusion' within the brain*. Annals of the New York Academy of Sciences **531**, 29-39 (1988)
- [21] A. Van Harreveld: *The extracellular space in the vertebrate central nervous system*. The Structure and Function of Nervous Tissue. Ed Bourne GH, Academic Press, New York, pp. 447-511 (1972)
- [22] J. P. Kinney, J. Spacek, T. M. Bartol, C. L. Bajaj, K. M. Harris, T. J. Sejnowski: *Extracellular sheets and tunnels modulate glutamate diffusion in hippocampal neuropil*. J Comp Neurol **521**, 448-464 (2013)
- [23] C. Nicholson, E. Sykova: *Extracellular space structure revealed by diffusion analysis*. Trends Neurosci **21**, 207-215 (1998)

- [24] A. M. Arranz, K. L. Perkins, F. Irie, D.P. Lewis, J. Hrabe, F. Xiao, N. Itano, K. Kimata, S. Hrabetova, Y. Yamaguchi: *Hyaluronan deficiency due to Has3 knock-out causes altered neuronal activity and seizures via reduction in brain extracellular space*. *J Neurosci* **34**, 6164–6176 (2014)
- [25] A. D. Sherpa, P. van de Nes, F. Xiao, J. Weedon, S. Hrabetova S: *Gliotoxin-induced swelling of astrocytes hinders diffusion in brain extracellular space via formation of dead-space microdomains*. *Glia* **62**, 1053-1065 (2014)
- [26] G. Kaur, S. Hrabetova, D. N. Guilfoyle, C. Nicholson, J. Hrabe: *Characterizing molecular probes for diffusion measurements in the brain*. *J Neurosci Methods* **171**, 218-25 (2008)
- [27] A. Reichenbach, H. Wolburg: *Astrocytic swelling in neuropathology*. In: *Neuroglia* (Kettenmann HO, Ransom BR, eds), p 521-531. New York: Oxford University Press (2005)
- [28] D. T. Theodosis, D. A. Poulain, S. H. R. Oliet: *Activity-dependent structural and functional plasticity of astrocyte-neuron interactions*. *Physiol Rev* **88**, 983-1008 (2008)
- [29] M. E. Carter, O. Yizhar, S. Chikahisa, H. Nguyen, A. Adamantidis, S. Nishino, K. Deisseroth, L. de Lecea: *Tuning arousal with optogenetic modulation of locus coeruleus neurons*. *Nat Neurosci* **13**, 1526–1533 (2010)
- [30] C. M. Constantinople, R. M. Bruno: *Effects and mechanisms of wakefulness on local cortical networks*. *Neuron* **69**, 1061-1068 (2011)
- [31] C. Aoki: *Beta-adrenergic receptors: astrocytic localization in the adult visual cortex and their relation to catecholamine axon terminals as revealed by electron microscopic immunocytochemistry*. *J Neurosci* **12**, 781-792 (1992)
- [32] C. D. Tweedle, G. I. Hatton: *Ultrastructural comparison of neurons of supraoptic and circularis nuclei in normal and dehydrated rats*. *Brain Res Bul* **1**, 103-121 (1976)
- [33] C. D. Tweedle, G. I. Hatton: *Ultrastructural changes in rat hypothalamic neurosecretory cells and their associated glia during minimal dehydration and rehydration*. *Cell Tissue Res* **181**, 59-72 (1997)
- [34] D. T. Theodosis, D. A. Poulain, J. D. Vincent: *Possible morphological bases for synchronization of neuronal firing in the rat supraoptic nucleus during lactation*. *Neuroscience* **6**:919-929 (1981)
- [35] D. Theodosis, D. A. Poulain: *Activity-dependent neuronal-glia and synaptic plasticity in the adult mammalian hypothalamus*. *Neuroscience* **57**, 501-535 (1993)
- [36] G. I. Hatton: *Function-related plasticity in the hypothalamus*. *Annual Review of Neuroscience* **20**, 375-397 (1997)
- [37] R. Piet, L. Vargova, E. Sykova, D. A. Poulain, S. H. R. Oliet: *Physiological contribution of the astrocytic environment of neurons to intersynaptic crosstalk*. *PNAS* **101**, 2151-2155 (2004)
- [38] A. Frigeri, M. A. Gropper, F. Umenishi, M. Kawashima, D. Brown, A. S. Verkman: *Localization of MIWC and GLIP water channel homologs in neuromuscular, epithelial and glandular tissues*. *J Cell Sci* **108**, 2993–3002 (1995)
- [39] S. Nielsen, E. A. Nagelhus, M. Amiry-Moghaddam, C. Bourque, P. Agre, O. P. Ottersen: *Specialized membrane domains for water transport in glial cells: high-resolution immunogold cytochemistry of aquaporin-4 in rat brain*. *J Neurosci* **17**, 171–180 (1997)
- [40] G. T. Manley, D. K. Binder, M. C. Papadopoulos, A. S. Verkman: *New insights into water transport and edema in the central nervous system from phenotype analysis of aquaporin-4 null mice*. *Neurosci* **129**, 983–991 (2004)
- [41] X. Yao, S. Hrabetova, C. Nicholson, G. T. Manley: *Aquaporin-4-deficient mice have increased extracellular space without tortuosity change*. *J Neurosci* **28**, 5460-5464 (2008)
- [42] D. K. Binder, X. Yao, Z. Zador, T. J. Sick, A. S. Verkman, G. T. Manley GT: *Increased seizure duration and slowed potassium kinetics in mice lacking aquaporin-4 water channels*. *Glia* **53**, 631–636 (2006)
- [43] L. Dmytrenko, M. Cicanic, M. Anderova, I. Vorisek, O. P. Ottersen, E. Sykova, L. Vargova: *The impact of alpha-syntrophin deletion on the changes in tissue structure and extracellular diffusion associated with cell swelling under physiological and pathological conditions*. *PLoS ONE* **8**, 1-12 (2013)



- [44] M. Aschner, J. W. Allen, H. K. Kimelberg, R. M. LoPachin, W. J. Streit: *Glial cells in neurotoxicity development*. *Annu Rev Pharmacol Toxicol* **39**, 151-173 (1999)
- [45] H.K. Kimelberg: *Astrocytic swelling in cerebral ischemia as a possible cause of injury and target for therapy*. *Glia* **50**, 389-397 (2005)
- [46] A. A. Mongin, H. K. Kimelberg: *Astrocytic swelling in neuropathology*. In: *Neuroglia* (Kettenmann HO, Ransom BR, eds), p 521-531. New York: Oxford University Press (2005)
- [47] M. E. Rice, C. Nicholson: *Diffusion characteristics and extracellular volume fraction during normoxia and hypoxia in slices of rat neostriatum*. *J Neurophysiol* **65**, 264-272 (1991)
- [48] M. A. Pérez-Pinzón, L. Tao, C. Nicholson: *Extracellular potassium, volume fraction, and tortuosity in rat hippocampal CA1, CA3, and cortical slices during ischemia*. *J Neurophysiol* **74**, 565-573 (1995)
- [49] G. C. Newman, F. E. Hospod, P. Wu: *Thick brain slices model the ischemic penumbra*. *J Cereb Blood Flow Metab* **8**, 586-597 (1988)
- [50] S. Hrabetova, C. Nicholson: *Dextran decreases extracellular tortuosity in thick-slice ischemia model*. *J Cereb Blood Flow Metab* **20**, 1306-1310 (2000)
- [51] E. Sykova, J. Svoboda, J. Polak, A. Chvatal: *Extracellular volume fraction and diffusion characteristics during progressive ischemia and terminal anoxia in the spinal cord of the rat*. *J Cereb Blood Flow Metab* **14**, 301-311 (1994)
- [52] I. Vorisek, E. Sykova: *Ischemia-induced changes in the extracellular space diffusion parameters,  $K^+$ , pH in the developing rat cortex and corpus callosum*. *J Cereb Blood Flow Metab* **17**, 191-203 (1997)
- [53] A. Van Harreveld, S. K. Malhotra: *Extracellular space in the cerebral cortex of the mouse*. *J Anat* **101**, 197-207 (1967)
- [54] J. R. Stiles, T. M. Bartol: *Monte Carlo methods for simulation realistic synaptic micro physiology using MCell*. In: *Computational Neuroscience: Realistic Modeling for Experimentalists* (De Schutter E, eds), p 87-127. London: CRC (2001)
- [55] A. W. El-Kareh, S. L. Braunstein, T. W. Secomb: *Effect of cell arrangement and interstitial volume fraction on the diffusivity of monoclonal antibodies in tissue*. *Biophys J* **64**, 1638-1646 (1993)
- [56] L. Tao, C. Nicholson: *Maximum geometrical hindrance to diffusion in brain extracellular space surrounding uniformly spaced convex cells*. *J Theor Biol* **229**, 59-68 (2004)
- [57] A. Tao, L. Tao, C. Nicholson: *Cell cavities increase tortuosity in brain extracellular space* *J Theor Biol* **234** 525-536 (2005)
- [58] S. Hrabetova: *Extracellular diffusion is fast and isotropic in the stratum radiatum of hippocampal CA1 region in rat brain slices*. *Hippocampus* **15**, 441-450 (2005)
- [59] G. T. Manley, M. Fujimura, T. Ma, N. Noshita, F. Filiz, A. W. Bollen, P. Chan, A. S. Verkman: *Aquaporin-4 deletion in mice reduces brain edema after acute water intoxication and ischemic stroke*. *Nat Med* **6**, 159-163 (2000)
- [60] X. Yao, N. Derugin, G. T. Manley, A. S. Verkman: *Reduced brain edema and infarct volume in aquaporin-4 deficient mice after transient focal cerebral ischemia*. *Neurosci Lett* **584**, 368-372 (2015)
- [61] M. Weller: *Gliomas*. In: *Neuroglia* (Kettenmann HO, Ransom BR, eds), p 550-562. New York: Oxford University Press (2005)
- [62] L. Vargova, A. Homola, J. Zamecnik, M. Tichy, V. Benes, E. Sykova: *Diffusion parameters of the extracellular space in human gliomas*. *Glia* **42**, 77-88 (2003)
- [63] L. Bakay: *The extracellular space in brain tumours.I. Morphological considerations*. *Brain* **93**, 693-698 (1970)
- [64] L. Bakay: *The extracellular space in brain tumours.II. The sucrose space*. *Brain* **93**, 699-708 (1970)
- [65] J. Zamecnik: *The extracellular space and matrix of gliomas*. *Acta Neuropathol* **110**, 435-442 (2005)
- [66] J. Zamecnik, L. Vargova, A. Homola, R. Kodet, E. Sykova: *Extracellular matrix glycoproteins and diffusion barriers in human astrocytic tumours*. *Neuropathol Appl Neurobiol* **30**, 338-350 (2004)
- [67] C. Nicholson, L. Tao: *Hindered diffusion of high molecular weight compounds in brain extracellular microenvironment measured with integrative optical imaging*. *Biophys J* **65**, 2277-2290 (1993)

[68] A. Saghyan, D. P. Lewis, J. Hrabec, S. Hrabetova: *Extracellular diffusion in laminar brain structures exemplified by hippocampus*. J Neurosci Methods **205**, 110-118 (2012)